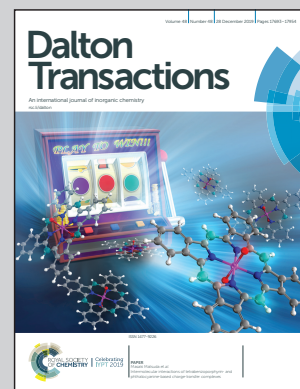


Showcasing research from Professor Garcia's laboratory, Institute of Chemical Technology, Technical University of Valencia, Spain.

Subphthalocyanine encapsulated within MIL-101(Cr)-NH₂ as a solar light photoredox catalyst for dehalogenation of α -haloacetophenones

The figure illustrates a molecule of subphthalocyanine attached to the MIL-101 structure and how light can activate it to promote dehalogenation and coupling.

As featured in:



See Hermenegildo Garcia et al., *Dalton Trans.*, 2019, 48, 17735.

Cite this: *Dalton Trans.*, 2019, **48**, 17735

Subphthalocyanine encapsulated within MIL-101(Cr)-NH₂ as a solar light photoredox catalyst for dehalogenation of α -haloacetophenones†

Andrea Santiago-Portillo,^a Sonia Remiro-Buenamañana,^b Sergio Navalón^a and Hermenegildo García *^{a,b,c}

Subphthalocyanine has been incorporated into a robust metal–organic framework having amino groups as binding sites. The resulting SubPc@MIL-101(Cr)-NH₂ composite has a loading of 2 wt%. Adsorption of subphthalocyanine does not deteriorate host crystallinity, but decreases the surface area and porosity of MIL-101(Cr)-NH₂. The resulting SubPc@MIL-101(Cr)-NH₂ composite exhibits a 575 nm absorption band responsible for the observed photoredox catalytic activity under simulated sunlight irradiation for hydrogenative dehalogenation of α -haloacetophenones and for the coupling of α -bromoacetophenone and styrene. The material undergoes a slight deactivation upon reuse. In comparison to the case of phthalocyanines the present study is one of the few cases showing the use of subphthalocyanine as a photoredox catalyst, with its activity derived from site isolation within the MOF cavities.

Received 11th October 2019,
Accepted 11th November 2019

DOI: 10.1039/c9dt04004h

rsc.li/dalton

Introduction

Metal–organic frameworks (MOFs) are currently among the most intensely studied photocatalysts due to the efficient photoinduced electron transfer from the excited linker to the metal nodes.^{1–9} However, very frequently organic linkers do not show photoresponse under visible light irradiation and different strategies have been developed to expand MOF photoresponse to the visible region. Among them, the strategy that has been widely used is the substitution of an aromatic linker with amino groups that introduce a new $n \rightarrow \pi^*$ electronic transition with an onset at about 450 nm.² However, in most of the cases, amino group substitution does not expand the photoresponse towards the red beyond 450 nm. For this reason, alternative strategies consisting of the anchoring of the peripheral framework positions of additional chromophores or metallic complexes such as ruthenium(II) polypyridyl complexes have also been applied.^{1,2,5} In this context, although MOFs with phthalocyanine units as organic linkers have been

well-established as photocatalysts,¹⁰ the use of subphthalocyanines has so far not been reported in spite of the intense absorption band that these macrocyclic dyes exhibit in the visible region.^{11–13}

In the present study, the preparation of MIL-101(Cr)-NH₂ containing subphthalocyanine (SubPc@MIL-101(Cr)-NH₂) as a visible light harvester unit has been described. This composite exhibits activity for the sunlight photoredox catalytic hydrogenative debromination of bromoacetophenone in the presence of electron donors (photoredox reaction).¹⁴

Results and discussion

Photocatalyst preparation and characterization

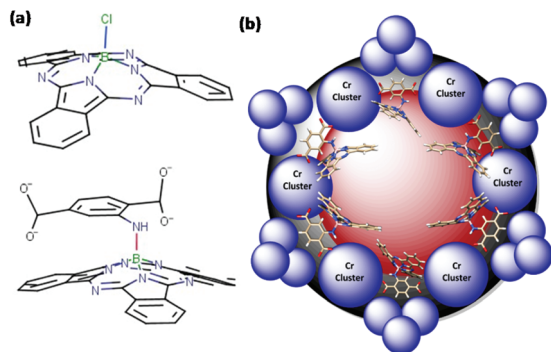
MIL-101(Cr)-NH₂ was selected in the present study as a host for SubPc-Cl for various reasons, including framework robustness, the presence of –NH₂ groups as apical binding sites for SubPc-Cl, large porosity, high surface area and reliable synthesis.^{15–17} The amino groups present in the terephthalate linkers are expected to act as binding sites for the apical position of SubPc-Cl, replacing Cl[–].^{18,19} It is expected that the substitution of Cl[–] in SubPc-Cl by the amino groups located in the MOF cavities would result in the formation of a strongly bound composite that could exhibit visible light photoresponse due to the optical properties of SubPc.^{20–23} Therefore, MIL-101(Cr)-NH₂ appears to be a preferred porous host to incorporate SubPc-Cl in comparison to the parent

^aDepartamento de Química, Universitat Politècnica de València, C/Camino de Vera, s/n, 46022 Valencia, Spain. E-mail: hgarcia@qim.upv.es

^bInstituto Universitario de Tecnología Química, CSIC-UPV, Universitat Politècnica de València, Av. de los Naranjos, Valencia 46022, Spain

^cCenter of Excellence for Advanced Materials Research, King Abdulaziz University, Jeddah, Saudi Arabia

† Electronic supplementary information (ESI) available: Additional characterization and catalytic data. See DOI: 10.1039/C9DT04004H



Scheme 1 (a) The structure of SubPc-Cl and its covalent linkage (red bond) with the -NH_2 groups present in the terephthalate organic ligand of MIL-101(Cr)- NH_2 ; (b) a cartoon illustrating the structure of SubPc@MIL-101(Cr)- NH_2 (red sphere: pore; blue spheres: Cr clusters; and black sphere: MIL101(Cr)- NH_2). Note that the NH_2 groups in terephthalate linkers play the role of apical coordination sites for SubPc.

MIL-101(Cr), in which such binding groups in the MOF linkers are not present. Scheme 1 illustrates the incorporation procedure and the anchoring of SubPc-Cl through the -NH_2 substituents.

After incorporation of SubPc-Cl into MIL-101(Cr)- NH_2 , isothermal gas adsorption measurements reveal a large decrease in the surface area value and a diminution of the porosity (Table 1).

The amount of SubPc adsorbed on MIL-101(Cr)- NH_2 was estimated by the combustion elemental analysis of carbon and nitrogen and from the comparison of the thermogravimetric profiles of MIL-101(Cr)- NH_2 and SubPc@MIL-101(Cr)- NH_2 . The data are also given in Table 1, while Fig. S1 in the ESI† shows the thermogravimetric profiles of these two solids, where it can be seen that the percentage of residual weight after decomposition of the organic components is larger for SubPc@MIL-101(Cr)- NH_2 as compared to MIL-101(Cr)- NH_2 . Analytical data indicate that the percentage of the subphthalocyanine guest in the composite material corresponds to about 2 wt%.

The XRD pattern of SubPc@MIL-101(Cr)- NH_2 is coincident with that of MIL-101(Cr)- NH_2 , indicating that the crystal structure of the MOF is preserved upon adsorption of SubPc-Cl. The absence of characteristic peaks corresponding to SubPc-Cl in the XRD pattern of the SubPc@MIL-101(Cr)- NH_2 composite indicates that no crystals of the boron macrocycle are detectable in the guest, this being compatible with site isolation of individual SubPc macrocycles inside the host cavities (Fig. 1).

Table 1 Isothermal N_2 adsorption and relevant elemental analysis of MIL-101(Cr)- NH_2 and SubPc@MIL-101(Cr)- NH_2

	MIL-101(Cr)- NH_2	SubPc@MIL-101(Cr)- NH_2
BET surface area ($\text{m}^2 \text{g}^{-1}$)	1950	490
Pore volume ($\text{cm}^3 \text{g}^{-1}$)	2	0.6
N (%)	3.2	4.9
C (%)	22.2	32.1

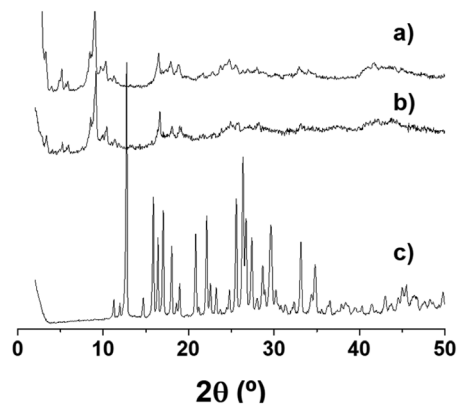


Fig. 1 The XRD patterns of (a) MIL-101(Cr)- NH_2 , (b) SubPc@MIL-101(Cr)- NH_2 and (c) SubPc-Cl.

The presence of SubPc as the guest incorporated into MIL-101(Cr)- NH_2 can be assessed by using diffuse reflectance UV-vis absorption spectra, in which the presence of a new band with a λ_{max} of about 570 nm, attributable to the presence of SubPc, can be observed. Fig. 2 shows a comparison of the diffuse reflectance UV-vis spectra of MIL-101(Cr)- NH_2 and those of the composite SubPc@MIL-101(Cr)- NH_2 . Fig. S2† shows the diffuse reflectance UV-visible spectra of SubPc-Cl. Comparison of the visible band corresponding to the occluded SubPc with that of the parent SubPc-Cl shows a clear red shift of the adsorption band from 495 to 575 nm. This notable shift can be attributed to the exchange of chloride as an apical ligand with the aromatic amino group, in agreement with the success of SubPc-Cl adsorption by strong interaction with the amino groups.

Coincident conclusions can be achieved by the analysis of the peaks corresponding to the different elements in XPS. Fig. 3 summarizes the most characteristic data obtained by XPS, while Fig. S3–S5 in the ESI† provide additional infor-

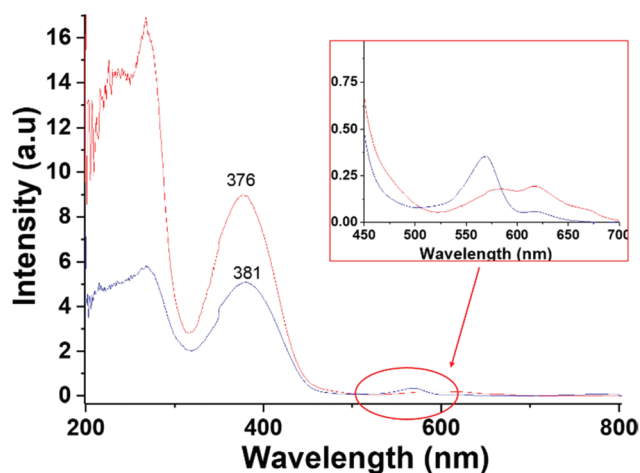


Fig. 2 The diffuse reflectance UV-vis spectra of MIL-101(Cr)- NH_2 (red line) and SubPc@MIL-101(Cr)- NH_2 (blue line).

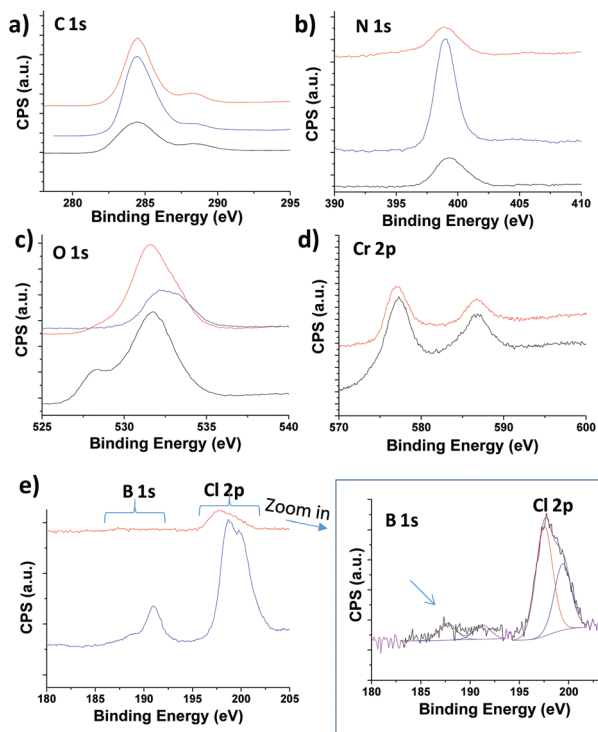


Fig. 3 XPS spectra of MIL-101(Cr)-NH₂ (black line), SubPc@MIL-101(Cr)-NH₂ (red line) and SubPc-Cl (blue line).

mation on the XPS peaks for each element. The most salient feature detected by XPS analysis is the observation of additional signals for B 1s and Cl 2p present in the SubPc@MIL-101(Cr)-NH₂ composite with respect to the pristine MIL-101(Cr)-NH₂ host, indicating the presence of SubPc in the material. Interestingly, the B 1s peak is split into two individual components that can be attributed to B atoms interacting with the amino groups of the linker and with the Cl⁻ anions. This interpretation agrees with the presence of Cl in the SubPc@MIL-101(Cr)-NH₂ composite, indicating that no complete replacement of the apical Cl ligand by NH₂ has occurred during the adsorption.

Photoredox catalysis

As commented in the introduction, the purpose of this study was to show that the adsorption of SubPc-Cl onto MIL-101(Cr)-NH₂ as a light harvesting centre affords photoredox activity with enhanced visible light photoresponse for hydrogenative debromination of α -bromoacetophenone (Fig. 4a).

Initial experiments were carried out with simulated sunlight in acetonitrile using triethanolamine (TEOA) as the electron donor. The results of the photoredox test are presented in Fig. 4. As can be seen in this figure, while negligible conversion is observed in the absence of any photocatalyst, the use of MIL-101(Cr)-NH₂ results only in 15% debromination at 8 h of irradiation. In contrast, using SubPc@MIL-101(Cr)-NH₂ as the photoredox catalyst, a complete conversion of

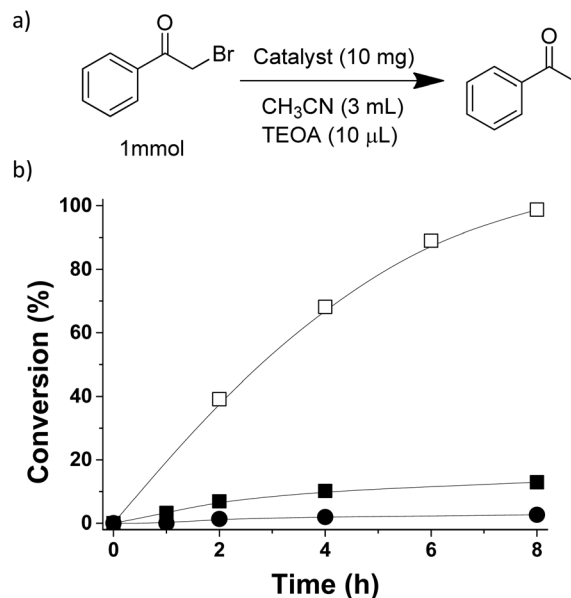


Fig. 4 The time-conversion plot of the hydrogenative debromination of α -bromoacetophenone to acetophenone using (■) MIL-101(Cr)-NH₂, (□) SubPc@MIL-101(Cr)-NH₂ and (●) without any catalyst. Reaction conditions: α -bromoacetophenone (1 mmol), TEOA (10 μ L), CH₃CN (3 mL) and MOF (10 mg, 5.1×10^{-4} mmol SubPc).

α -bromoacetophenone into acetophenone was achieved this time. It should be noted that the reaction does not take place in the dark, without visible light irradiation.

The photoredox stability of the composite was studied by performing consecutive runs. Fig. 5 shows the temporal profiles of the photoredox debromination activity upon reuse of the same SubPc@MIL-101(Cr)-NH₂ sample. The results show that the photoredox activity is maintained with only a slight decay from 90 to 83% after 4 uses.

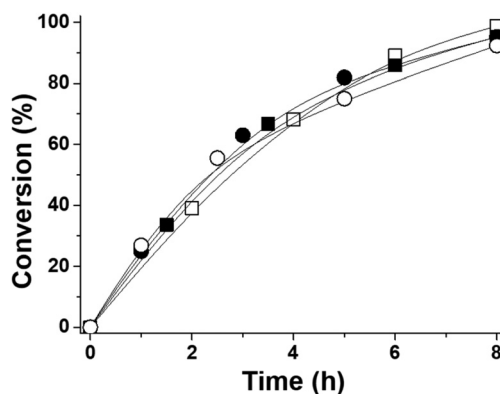


Fig. 5 The time-conversion plot of the hydrogenative debromination of α -bromoacetophenone to acetophenone upon consecutive reuses using SubPc@MIL-101(Cr)-NH₂ as a photoredox catalyst. Legend: (■) 1st use (□) 2nd use, (●) 3rd use and (○) 4th use. Reaction conditions: α -Bromoacetophenone (1 mmol), TEOA (10 μ L), CH₃CN (3 mL) and MOF (10 mg, 5.1×10^{-4} mmol SubPc).

The SubPc@MIL-101(Cr)-NH₂ composite was also efficient at promoting α -dechlorination of chloroacetophenone, although comparison of the temporal profiles of the bromo- and chloro-derivatives shows that the reaction is slower in the case of α -chloroacetophenone, in accordance with the higher bond strength of C–Cl with respect to C–Br. Fig. S6 in the ESI† shows a comparison of the photocatalytic activity for dechlorination with respect to debromination.

The fact that the reaction mechanism involves the generation of the α -ketyl radicals was confirmed by quenching of these radicals by 2,2,4,4-tetramethylpiperidinyloxy (TEMPO). Thus, if the photoredox debromination under simulated sunlight irradiation using the SubPc@MIL-101(Cr)-NH₂ composite is started under conventional reaction conditions and then after 2 h of reaction, TEMPO is added to the reaction mixture no further progress in the formation of acetophenone is observed. Fig. S7† compares the temporal profiles of the photocatalytic debromination in the absence and in the presence of TEMPO.

Finally, the solar light photoresponse of SubPc@MIL-101(Cr)-NH₂ was also applied for the photocatalytic coupling of α -bromoacetophenone and styrene to form α -phenylbutyrophenone, by irradiating with simulated sunlight. In this photoredox reaction, the α -ketyl radical should add to the C=C double bond of styrene, since this vinylic substrate can easily undergo attack by radicals as previously reported.²⁵ It is interesting to note that although the conversion was not high, the selectivity for α -phenylbutyrophenone was almost complete. It should be mentioned that also in this case the reaction does not occur in the dark without visible light irradiation. Fig. 6 shows the temporal profile of butyrophenone formation.

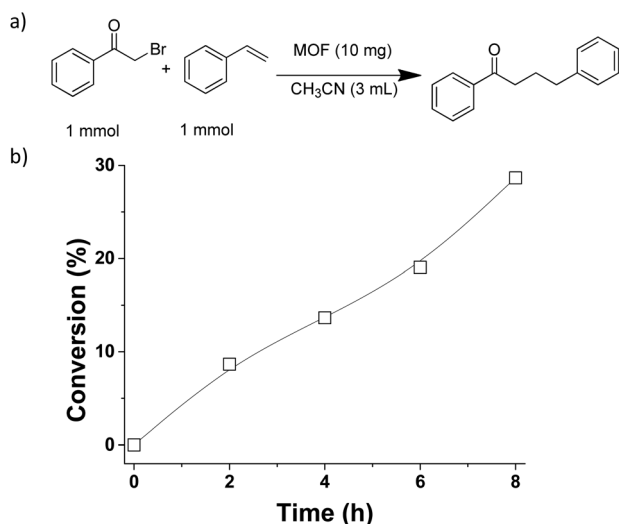


Fig. 6 The time-conversion plot of the coupling of α -bromoacetophenone and styrene using SubPc@MIL-101(Cr)-NH₂ as a photoredox catalyst. Reaction conditions: α -Bromoacetophenone (1 mmol), styrene (1 mmol), CH₃CN (3 mL) and MOF (10 mg, 5.1×10^{-4} mmol SubPc).

Experimental

Materials

All the reagents and solvents used in the present paper were of analytical or HPLC grade and supplied by Sigma-Aldrich.

Catalyst preparation

MIL-101(Cr)-NH₂ preparation: MIL-101(Cr)-NO₂ was prepared following already reported procedures.^{16,17} Briefly, nitroterephthalic acid (1.5 mmol) and CrCl₃ (1 mmol) were introduced into a Teflon autoclave containing demineralized water (8 mL). Then, the autoclave was heated at 180 °C for 120 h. Once the autoclave was cooled to room temperature, the precipitate formed in the process was washed several times with dimethylformamide (DMF) at 120 °C and then with ethanol at 80 °C. Then, MIL-101(Cr)-NO₂ was subjected to post-synthetic modification using SnCl₂·H₂O as the reducing agent leading to the formation of MIL-101(Cr)-NH₂ according to reported procedures.^{16,17}

SubPc@MIL101(Cr)-NH₂ preparation: boron chloride subphthalocyanine (SubPc-Cl) was synthesized following reported literature procedures.^{18,24} Then, MIL101(Cr)-NH₂ (60 mg) was thermally activated by heating at 150 °C under vacuum in a 3 necked round bottomed flask connected to a reflux condenser for 22 h. SubPc-Cl (6 mg) was dissolved in dry toluene (6 mL) and the solution was added to the flask containing the active MOF. The suspension was then refluxed under an inert atmosphere for 48 h. The dispersion was filtered under vacuum and washed with toluene, and the resulting solid was subsequently subjected to Soxhlet extraction using chloroform (150 mL) as solvent for 12 h.

Catalyst characterization

Powder X-ray diffraction (PXRD) of the materials was performed on a Philips XPert diffractometer equipped with a graphite monochromator (40 kV and 45 mA) employing Ni filtered CuK α radiation. N₂ adsorption isotherms at 77 K were recorded using a Micromeritics ASAP 2010 device. Thermogravimetric analyses were performed on a TGA/SDTA851e METTLER TOLEDO station. The X-ray photoelectron spectra (XPS) of different solids were collected on a SPECS spectrometer equipped with a MCD-9 detector using a monochromatic Al (K_{α} = 1486.6 eV) X-ray source for calibrating the binding energy based on the C 1s peak set at 284.4 eV as reference. CASA software has been employed for spectral deconvolution. Diffuse reflectance UV-visible spectra were recorded using a Cary 5000 Varian spectrophotometer having an integrating sphere; the sample as compressed powder was placed in a sample holder.

Catalytic experiments

The required amount of catalyst (10 mg) was introduced into a quartz tube containing acetonitrile (3 mL) dissolved in α -bromoacetophenone (1 mmol) and TEOA (10 μ L) and the system was purged with Ar. Then, the tube was irradiated with a solar simulator. The reactions were magnetically stirred and

reaction aliquots were sampled at the corresponding reaction times.

In the reusability experiments, the SubPc@MIL-101(Cr)-NH₂ solid was recovered at the end of the reaction by filtration (nylon filter, 0.2 μm). Then, the catalyst was transferred to a round-bottom flask (50 mL) and subjected to ethanol washing (20 mL) under magnetic stirring for 30 min. This procedure was repeated two more times. The final solid was recovered by filtration (nylon filter, 0.2 μm) and dried in an oven.

The coupling of α-bromoacetophenone and styrene was performed by dissolving 10 mg of the catalyst in 3 mL of acetonitrile containing 1 mmol of α-bromoacetophenone and 1 mmol of styrene. The solution was placed in a quartz test tube sealed with a septum cap. Then, the system was purged with argon. Subsequently, the reaction tube was irradiated with a solar simulator. The reaction was magnetically stirred and reaction aliquots were sampled at the corresponding reaction times.

Product analysis

Previously filtered reaction aliquots were diluted in an acetonitrile solution containing a known amount of nitrobenzene as the external standard. The aliquots were immediately analyzed by gas chromatography (GC) using a flame ionization detector. Quantification was carried out based on calibration plots obtained with authentic samples against nitrobenzene. Reaction products were identified using a GC (Hewlett Packard HP6890 Chromatograph) coupled to a mass spectrometer (MS, Agilent 5973). In addition, acetophenone formation was confirmed by co-injection in the gas chromatograph with a commercial sample.

Conclusions

The present study shows that adsorption of subphthalocyanine at a loading of about 2 wt% inside a robust MOF having amino groups in the terephthalate linker as binding sites renders a composite with solar light photoresponse that is able to promote hydrogenative dehalogenation of α-haloacetophenones. The reaction involves ketyl radicals and the catalyst can be reused with only minor decay in its photocatalytic activity. Since compared to related phthalocyanines, subphthalocyanines have been much less used as light harvesters and photosensitizers, the present study illustrates the potential that this boron macrocycle can have in photoredox catalysis.

Conflicts of interest

There are no conflicts to declare.

Acknowledgements

Financial support from the Spanish Ministry of Economy and Competitiveness (Severo Ochoa and RTI2018-098237-B-C21)

and Generalitat Valenciana (Prometeo 2017-083) is gratefully acknowledged. S. N. is thankful for the financial support from the Fundación Ramón Areces (XVIII Concurso Nacional para la Adjudicación de Ayudas a la Investigación en Ciencias de la Vida y de la Materia, 2016), the Ministerio de Ciencia, Innovación y Universidades RTI 2018-099482-A-I00 project and the Generalitat Valenciana grupos de investigación consolidables 2019 (ref: AICO/2019/214) project. S. R.-B. also thanks the Research Executive Agency (REA) and the European Commission for the funding received under the Marie Skłodowska Curie actions (H2020-MSCA-IF-2015/Grant agreement number 709023/ZESMO).

Notes and references

- X. Deng, Z. Li and H. García, *Chem. – Eur. J.*, 2017, **23**, 11189–11209.
- A. Dhakshinamoorthy, A. M. Asiri and H. García, *Angew. Chem., Int. Ed.*, 2016, **55**, 5414–5445.
- D. Jiang, P. Xu, H. Wang, G. Zeng, D. Huang, M. Chen, C. Lai, C. Zhang, J. Wan and W. Xue, *Coord. Chem. Rev.*, 2018, **376**, 449–466.
- R. Li, W. Zhang and K. Zhou, *Adv. Mater.*, 2018, **30**, 1705512.
- J. Qiu, X. Zhang, Y. Feng, X. Zhang, H. Wang and J. Yao, *Appl. Catal., B*, 2018, **231**, 317–342.
- L. Shen, R. Liang and L. Wu, *Chin. J. Catal.*, 2015, **36**, 2071–2088.
- Y. Shi, A.-F. Yang, C.-S. Cao and B. Zhao, *Coord. Chem. Rev.*, 2019, **390**, 50–75.
- S. Wang and X. Wang, *Small*, 2015, **11**, 3097–3112.
- M. Wen, K. Mori, Y. Kuwahara, T. An and H. Yamashita, *Chem. – Asian J.*, 2018, **13**, 1767–1779.
- S. Das and W. M. A. Wan Daud, *Renewable Sustainable Energy Rev.*, 2014, **39**, 765–805.
- B. del Rey, U. Keller, T. Torres, G. Rojo, F. Agulló-López, S. Nonell, C. Martí, S. Brasselet, I. Ledoux and J. Zyss, *J. Am. Chem. Soc.*, 1998, **120**, 12808–12817.
- C. G. Claessens, D. González-Rodríguez and T. Torres, *Chem. Rev.*, 2002, **102**, 835–853.
- N. Kobayashi, in *The Porphyrin Handbook*, ed. K. M. Kadish, K. M. Smith and R. Guilard, Academic Press, Amsterdam, 2003, pp. 161–262.
- A. Santiago-Portillo, H. G. Baldoví, E. Carbonell, S. Navalón, M. Alvaro, H. García and B. Ferrer, *J. Phys. Chem. C*, 2018, **122**, 29190–29199.
- G. Ferey, C. Mellot-Draznieks, C. Serre, F. Millange, J. Dutour, S. Surble and I. Margiolaki, *Science*, 2005, **309**, 2040–2042.
- A. Santiago-Portillo, J. F. Blandez, S. Navalón, M. Álvaro and H. García, *Catal. Sci. Technol.*, 2017, **7**, 1351–1362.
- A. Santiago-Portillo, S. Navalón, P. Concepción, M. Álvaro and H. García, *ChemCatChem*, 2017, **9**, 2506–2511.
- C. G. Claessens, D. Gonzalez-Rodriguez, M. S. Rodriguez-Morgade, A. Medina and T. Torres, *Chem. Rev.*, 2014, **114**, 2192–2277.

- 19 J. Guilleme, L. Martínez-Fernández, D. González-Rodríguez, I. Corral, M. Yáñez and T. Torres, *J. Am. Chem. Soc.*, 2014, **136**, 14289–14298.
- 20 M. Managa, J. Mack, D. Gonzalez-Lucas, S. Remiro-Buenamañana, C. Tshangana, A. N. Cammidge and T. Nyokong, *J. Porphyrins Phthalocyanines*, 2015, **20**, 1–20.
- 21 G. Bressan, A. N. Cammidge, G. A. Jones, I. A. Heisler, D. Gonzalez-Lucas, S. Remiro-Buenamañana and S. R. Meech, *J. Phys. Chem. A*, 2019, **123**, 5724–5733.
- 22 G. E. Morse and T. P. Bender, *ACS Appl. Mater. Interfaces*, 2012, **4**, 5055–5068.
- 23 K. L. Sampson, X. Jiang, E. Bukuroshi, A. Dovijarski, H. Raboui, T. P. Bender and K. M. Kadish, *J. Phys. Chem. A*, 2018, **122**, 4414–4424.
- 24 C. G. Claessens, D. Gonzalez-Rodriguez, B. del Ray, T. Torres, G. Mark, H.-P. Schuchmann, C. von Sonntag, J. G. MacDonald and R. S. Nohr, *Eur. J. Org. Chem.*, 2003, 2547–2551.
- 25 E. Speckmeier, P. J. W. Fuchs and K. Zeitler, *Chem. Sci.*, 2018, **9**(35), 7096–7103.